

# Photonic generation of W-band arbitrary waveforms with high time-bandwidth products enabling 3.9 mm range resolution: supplementary material

YIHAN LI,<sup>1,†</sup> AMIR RASHIDINEJAD,<sup>1,†</sup> JHIH-MIN WUN,<sup>2</sup> DANIEL E. LEAIRD,<sup>1</sup>  
JIN-WEI SHI,<sup>2</sup> ANDREW M. WEINER,<sup>1,\*</sup>

<sup>1</sup>School of Electrical and Computer Engineering, Purdue University, West Lafayette, Indiana, 47907, USA

<sup>2</sup>Department of Electrical Engineering, National Central University, Zhongli, 320, Taiwan

<sup>†</sup> These authors contributed equally to this work.

\*Corresponding author: [amw@purdue.edu](mailto:amw@purdue.edu)

Published 18 December 2014

This document provides supplementary information to “Photonic generation of W-band arbitrary waveforms with high time-bandwidth products enabling 3.9 mm range resolution,” <http://dx.doi.org/10.1364/optica.1.000446>, including details of the various procedures, methods and experimental components used in our W-band experiments, the results of which are presented in the main manuscript. Finally, a special in-depth elaboration of the phase-noise measurement setup and procedure as well as comparison with modern electronic arbitrary waveform generator is also provided. © 2014 Optical Society of America

<http://dx.doi.org/10.1364/optica.1.000446.soo1>

## Down-Conversion and Measurement Setup.

As depicted in Figs. 1(a) and 5(a), the down-conversion and measurement setup are the same for all reported experiments. At the receiver end, after a W-band low-noise amplifier (Millitech LNA-10-02150, 20 dB gain, ~5 dB noise figure), we must down-convert to be able to measure the generated signals using our 20 GHz real-time oscilloscope (Tektronix DSA72004B). The down-conversion stage is provided through a W-band 2nd-harmonic mixer (Virginia Diodes WR10SHM, ~17 GHz bandwidth, 7 dB conversion loss) which is driven by a local oscillator (Agilent E8257D-550) with frequency varied from 35 GHz to 50 GHz.

## Interferometric RF-AWG Experimental Setup.

An erbium-doped fiber-ring mode-locked laser with ~53 MHz repetition rate is used as the input source. To shape the pulses, we utilize a commercial pulse shaper (Finisar 1000S) with spectral resolution of ~10 GHz and operating wavelength of 1527.4 nm–1567.4 nm. The dispersive medium is simply a ~25 km spool of single mode fiber (SMF, total dispersion of ~393.6 ps/nm).

## Interferometric Generation of Linear Down-Chirp.

In order to generate a linear down-chirp covering 70–110 GHz, a quadratic phase-only function,  $\angle H(\omega) = 2e^{-24}\omega^2$ , is applied onto

the pulse shaper; while the variable delay is set to  $\tau = 283.5$  ps, corresponding to a center frequency of 90 GHz. The TBP of the generated waveform is maximally bound to the number of resolution pixels of the utilized optical pulse shaper, resulting in a TBP of 600.

## Phase Alignment.

In order to characterize waveforms with bandwidths beyond that of the mixer, measurements are performed sequentially with different local oscillator frequencies. Although the synthesizer LO frequencies are highly precise, their relative phases are not controlled. This results in phase misalignment in the down-converted waveforms measured with different LO frequencies. In order to combine these measurements to reconstruct the total waveform, phase alignment is required. This is carried out off-line by iteratively phase shifting each measurement (other than the first) and maximizing its cross-correlation with the first (reference) measurement.

## Calculation of Spectrogram.

The spectrogram of Fig. 2(d) was calculated numerically using the following:

$$S_e(f, \tau) = \left| \int e(t)g(t - \tau) e^{-j2\pi f t} dt \right|^2$$

where  $e(t)$  is the RF burst and  $g(t)$  a gating function. Here, the gating function is chosen to be Gaussian, that is,  $g(t) = \exp(-t^2/t_p^2)$  with  $t_p = 0.25$  ns. The squared magnitude of the fast Fourier transform (FFT) of the windowed RF signal was then computed to obtain the spectrogram. The function is further normalized before plotting.

### Interferometric Generation of Costas Sequence.

A Costas sequence of length 15 and fundamental frequency of 1 GHz is created about a 90 GHz ( $\tau = 283.5$ ) carrier frequency. The harmonic ordering for this sequence is tabulated below:

Length 15 Costas Sequence
Frequency Hop Sequence Ordering
7, 0*, -3, -5, 5, -7, -4, 2, 1, 3, 4, -1, 6, -2, -6
* Zero denotes no frequency shift

### Calculation of Auto-Ambiguity Function.

The auto-ambiguity function of Fig. 2(f) was calculated numerically using the following:

$$\chi(f, \tau) = \left| \int e(t)e^*(t - \tau) e^{-j2\pi f t} dt \right|^2$$

where  $e(t)$  is the RF burst. The function is further normalized before plotting.

### Arbitrary Long Repetition Period RF-AWG.

Pulses from a commercial mode-locked laser (Menlo Systems FC1500-250-WG) with 250 MHz repetition rate are switched to either arm according to a PN sequence using a complementarily driven pair of lithium niobate intensity modulators. Two commercial pulse shapers (Finisar 1000S, operating bandwidth of 40 nm) provide the pre-distorted anti-phase spectral shaping required for near-field-FTM. The spectrally-shaped pulses are then combined and directed through a  $\sim 3.3$  km long dispersive medium (SMF, total dispersion  $\sim 50$  ps/nm), corresponding to  $\sim 2$  ns time-aperture for each basis waveform.

### Ranging Procedure.

A reference waveform is first acquired using a real-time oscilloscope connected to the receive antenna with a single reflector placed in the beam path. The reference reflector may then be removed if desired, and targets are placed in the environment. The new waveform at the receiver is measured and cross-correlated offline with the reference. The obtained cross-correlations are plotted versus both round-trip time ( $\Delta t$ ) and range displacement with respect to the transceiver ( $\Delta z = c\Delta t/2$ , where  $c$  is the speed of light).

### Phase-Noise Measurement and Comparisons.

In order to make this measurement, we utilized the interferometric radio-frequency arbitrary waveform generation (RF-AWG) setup of Fig. 2(a), programmed to generate single-tone RF pulses at 80 GHz. The key components of this setup are: a self-referenced mode-locked fiber laser (Menlo Systems FC1500-250-WG, 250 MHz repetition rate, synchronized to a stable 10 MHz external clock); a high-resolution commercial pulse shaper (Finisar 1000S, 40 nm operating bandwidth, 10 GHz resolution);  $\sim 6.6$  km

of dispersive medium (SMF, total dispersion  $\sim 100$  ps/nm); and a high-speed near-ballistic uni-travelling-carrier photodiode (NBUTC-PD). The amount of dispersion is carefully fine-tuned such that 4 ns, 80 GHz waveform bursts, one from each mode-locked laser pulse, line up in phase with each other in a continuous

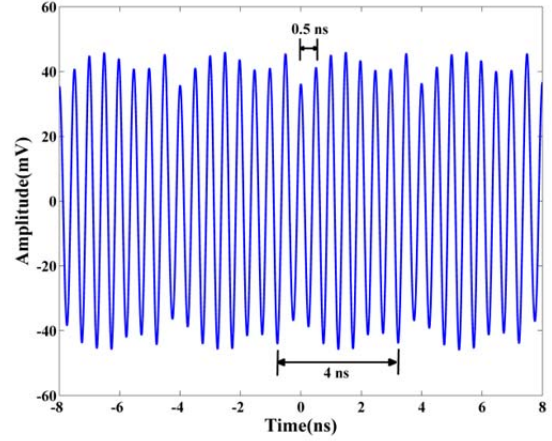


**Fig. S1.** Temporal profile of the down-converted 80 GHz waveform (LO =  $2 \times 39$  GHz).

fashion, thus artificially creating an almost continuous single-frequency RF tone at 80 GHz.

Since we were not able to measure this signal directly with the scope, the generated waveform was down-converted with a second-harmonic W-band mixer driven with a local oscillator (LO) signal set to 39 GHz (equivalent to 78 GHz down-conversion), as in Fig. 1(a). Setting the LO to 78 GHz allowed slightly higher conversion efficiency and harmonic extinction of about 15 dB. Moreover, the local oscillator was synchronized to the same stable 10 MHz clock signal that was used to synchronize the repetition rate of the mode-locked laser. Figure S1 depicts the temporal profile of the down-converted signal measured with a 20 GHz real-time oscilloscope. A near single frequency tone is clearly observed, although some modulation that repeats at the 4 ns laser period remains. The frequency of the measured signal in baseband is 2 GHz, which given the 78 GHz LO, corresponds to an original W-band signal at 80 GHz.

The down-converted 2 GHz signal was then directed to an RF spectrum analyzer, equipped with a phase-noise measurement utility. Single-sideband (SSB) phase-noise measurements are then carried out on this waveform from 10 Hz to 1 MHz using the following equation:

$$\mathcal{L}(f) = \frac{\text{Power within 1 Hz bandwidth at frequency } f}{\text{Total Signal Power}}$$

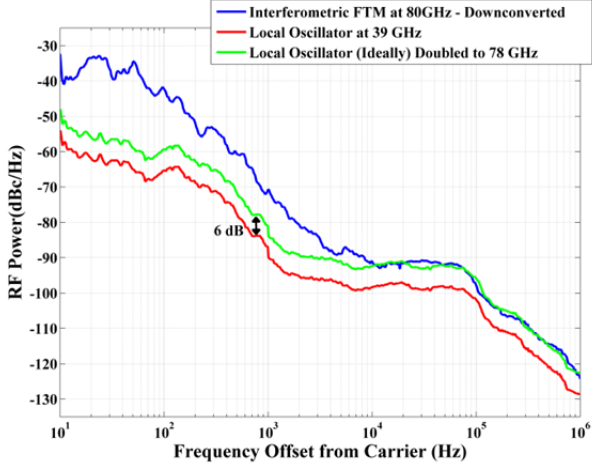


**Fig. S2.** Phase-noise measurements of the down-converted 80 GHz waveform (in blue), utilized LO frequency at 39 GHz (in red), and its ideal projection to 78 GHz (in green).

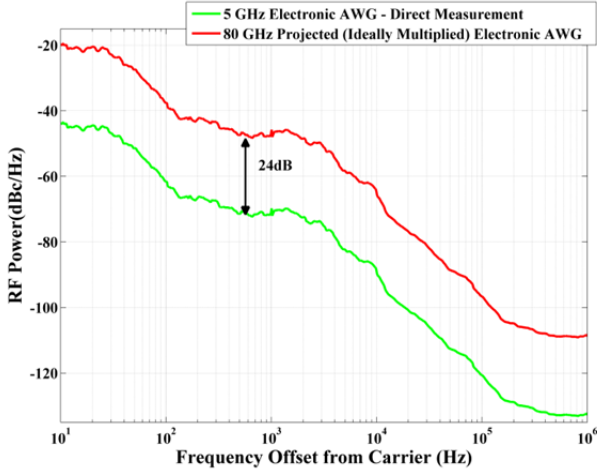


**Fig. S3.** Phase-noise measurement of a 5 GHz RF signal generated using state-of-the-art electronic AWG and its projection to 80 GHz assuming ideal up-conversion.

The result of phase-noise analysis on this down-converted signal is presented in Fig. S2, blue curve. It is necessary to emphasize again that the obtained plot is the phase-noise curve for the down-converted signal; the down-conversion stage may add to the phase-noise of the original 80 GHz signal. In order to achieve a better understanding of this effect, we also measured the phase-noise of the local oscillator (39 GHz) driving the mixer and overlaid it with the previous measurement in Fig. S2, red curve. Also, since we are using a second-harmonic mixer, ideally, the 78 GHz LO frequency should have  $20 \log_{10}(2) = 6$  dB higher phase-noise than the driving 39 GHz signal coming from the generator. This curve is also plotted in the same figure, Fig. S2 in green. It can be observed that after about 10 kHz, the curves for the down-converted 80 GHz and the 78 GHz LO fall on top of each other. This means that above approximately 10 kHz frequency offset, the phase-noise measured for the 80 GHz photonically-generated signal is dominated by the LO phase-noise.

Next, to provide comparison with modern electronic RF arbitrary waveform generator systems, we utilized a Tektronix AWG7000A (9.6 GHz analog bandwidth at 6 dB) and programed it to generate a continuous 5 GHz RF tone. We must note that due to the fact that the current state-of-the-art electronic AWG systems cannot generate W-band signals directly, we were forced to use

phase-noise measurements of this 5 GHz signal and project it to the W-band (namely 80 GHz) by assuming ideal up-conversion of this signal. Also, to provide a fair comparison, we clocked the electronic AWG device with the same stable 10 MHz used for our W-band generation and phase-noise measurements. Figure S3 shows the phase-noise curve of this 5 GHz waveform. In this plot, we have assumed ideal frequency multiplication effect on the phase-noise, meaning that this increase of  $20 \log_{10}(80 \text{ GHz} / 5 \text{ GHz}) = 24$  dB is the best case scenario when the 5 GHz signal is multiplied up to 80 GHz. In reality, the actual phase-noise could be higher.

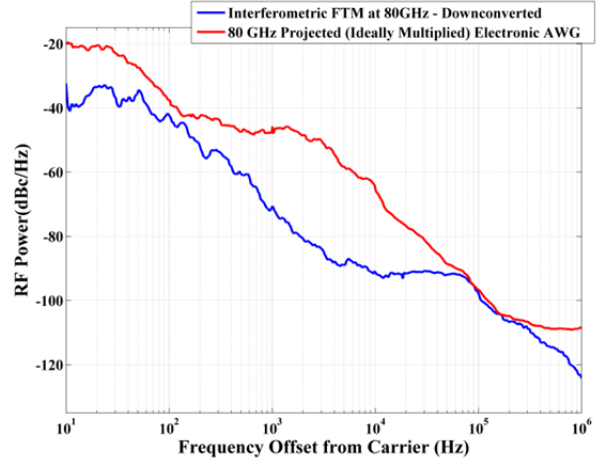


**Fig. S4.** Comparison between the projected phase-noise of state-of-the-art electronic AWG versus down-converted phase-noise of our photonic-assisted RF-AWG, both at 80 GHz.

Finally, Fig. S4 illustrates the projected phase-noise of the 80 GHz signal that would be generated from the frequency-multiplied electronic AWG overlaid with the phase-noise measurement of our photonic-assisted RF-AWG setup at the same 80 GHz frequency from Fig. S2. This plot clearly shows that our scheme's phase-noise of our photonic-assisted generation substantially outperforms that projected for a frequency-multiplied commercial electronic arbitrary waveform generator at all offset frequencies measured. According to the measurement, the phase-noise advantage of our scheme is as high as 35 dB (at  $\sim 3.5$  kHz offset). We reiterate that because our phase-noise measurement of the down-converted photonically generated 80 GHz signal is limited by the LO over much of the high frequency range, its actual phase-noise advantage may be even larger than suggested by Fig. S4.